High Energy Processes and Phenomena in Astrophysics
ASP Conference Series, Vol. , IAU Symposium 214

A High Angular Resolution View of Hot Gas in Clusters, Groups, and Galaxies – Mergers, Mixing, and Bubbling

W. Forman[1], E. Churazov[2,3], L. David[1], F. Durret[4], C. Jones[1], M. Markevitch[1], S. Murray[1], M. Sun[1], A. Vikhlinin[1,3]

[1]*Smithsonian Astrophysical Observatory, Cambridge, MA, USA*
[2]*MPI für Astrophysik, 85740 Garching, Germany*
[3]*Space Research Institute, 117997 Moscow, Russia*
[4]*Institut d'Astrophysique, 98bis Boulevard Arago, Paris, France*

Abstract.

We discuss two themes from Chandra and XMM-Newton observations of galaxies, groups, and clusters. First, we review observational aspects of cluster formation and evolution as matter accretes along filaments in A85 and A1367. We describe Chandra observations that probe the later evolutionary phases where the effects of mergers – both subsonic and supersonic – are observed in cluster cores as "cold fronts" and shocks. Second, we review the interactions between the hot, intracluster gas with relativistic plasma originating in active nuclei within the dominant galaxy at the cluster center. As examples of this interaction, we describe the radio and X-ray observations of M87 where buoyantly rising bubbles transfer energy and matter within the cluster core. We describe the Chandra observations of ZW3146 which exhibits both multiple cold fronts and relativistic plasma interactions. Finally, we describe the X-ray observations of NGC4636 where energy produced by the central AGN imprints a unique signature on the surrounding hot corona of the galaxy.

1. Cluster Evolution and Mergers

The most popular view of the formation of clusters, the largest gravitationally collapsed systems in the Universe, is that they form hierarchically from smaller mass systems at the nodes of large scale filaments. At the present epoch, matter continues to accrete onto clusters preferentially along the large scale filaments. X-ray observations of present epoch clusters, combined with optical studies, show both the large scale merging process as well as provide new insights into the detailed physics as merger remnants traverse cluster cores.

1.1. Filamentary Structures and Cluster Formation

A85 shows the effects of filamentary structure on the appearance of the cluster. In a remarkable ROSAT observation (Durret et al. 1998), a large scale X-ray filament was detected extending from a merging subcluster (South Blob) towards the southeast (see Fig. 1a) at a position angle of $\sim 160^\circ$ (measured from north, counterclockwise). The major axis of the central cD galaxy, the distribution

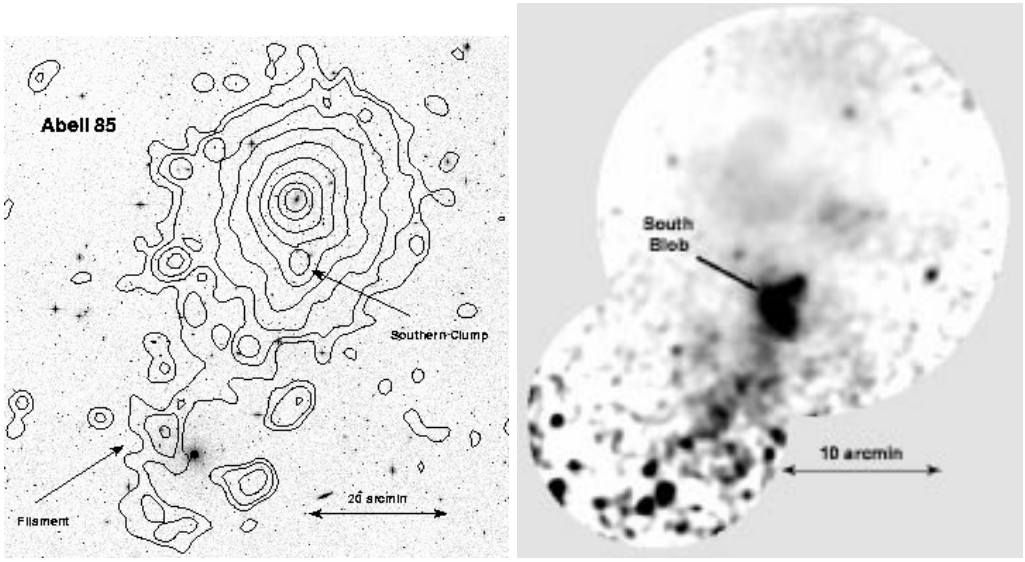

Figure 1. ROSAT and XMM-Newton observations of A85 (**a**) ROSAT PSPC iso-intensity contours (0.4-2.0 keV) are shown superposed on an optical image (adapted from Durret et al. 1998). A filamentary structure extends to the southeast. (**b**) The XMM-Newton MOS image shows the inner portion of the filament extending southeast from the South Blob (Southern Clump) (Durret et al. 2003).

of bright cluster galaxies, the X-ray filament and nearby groups and clusters all show a common orientation at this same $\sim 160^\circ$ angle over linear scales extending from 100 kpc (the outer isophotes of the central cD galaxy) to 25 Mpc, the alignment of nearby clusters (Durret et al. 1998). Such common alignments over a wide range of scales are expected if clusters form through accretion of matter from filaments and the accretion direction remains fixed over significantly long fractions of the age of the Universe (e.g., Van Haarlem & Van de Weygaert 1993). Recent XMM-Newton observations of A85 detect X-ray emission from the inner region of the filament extending from the southern clump ($10'$ south of the X-ray peak; see Fig. 1b) for about $15'$ to the southeast (Durret et al. 2003; see Kempner et al. 2002 for a discussion of the Chandra observation of the South Blob).

A second example of a cluster that clearly shows the importance of the surrounding filamentary structure is A1367. As shown by West & Blakeslee (2000), A1367 lies at the intersection of two filaments – the first extending roughly 100 Mpc from A1367 towards Virgo and the second extending between A1367 and Coma. The X-ray structure of A1367 as seen in the XMM-Newton observation in Fig. 2a and 2b shows effects from both these filaments with cool gas streaming into the cluster core from the direction of Coma to the northeast and a merger underway along the axis towards Virgo along the northwest–southeast axis (Forman et al. 2003a; see additional details on A1367 in the contribution by M. Sun in these proceedings).

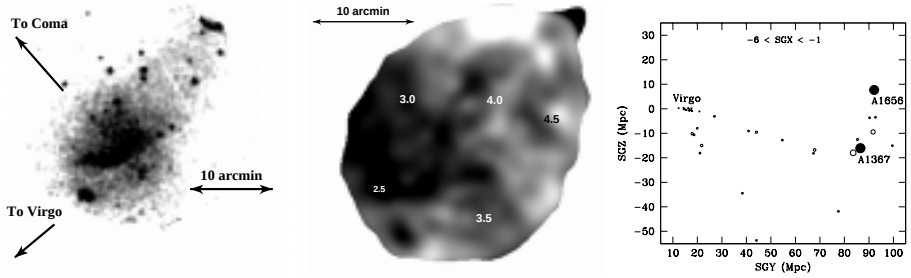

Figure 2. XMM-Newton observations of A1367 (Forman et al. 2003a) (**a**) Smoothed, flat-fielded, background-subtracted XMM-Newton (MOS) image shows the remarkable ellipticity of A1367 with the extension to the northwest. Also seen is the bright, highly structured core. (**b**) The temperature map (XMM-Newton MOS data) shows the extensive cool gas (darker shading is cooler gas; numbers indicate the gas temperature for the corresponding grey scale) entering the cluster from the east. (**c**) The large scale structure surrounding A1367 (adapted from West & Blakeslee 2000) shows filaments extending from A1367 towards the Virgo and Coma clusters.

A85 and A1367 contrast the effects of accretion. For A85, matter is accreting from a filament into a well-developed "cooling flow" cluster with a low entropy core centered on a cD galaxy. For A1367, we see accreting gas penetrating directly into the core of a less relaxed cluster.

1.2. Cold Fronts

The study of "cold fronts", contact discontinuities between cooler and hotter gas, began with the launch of Chandra (Markevitch et al. 2000; Vikhlinin et al. 2001a, b). A particularly revealing example of a cold front is seen in the Chandra observation of the Fornax cluster (Dosaj et al. 2002). In Fig. 3a, we see gas bound to the infalling bright elliptical galaxy NGC1404 as it approaches the cluster center (to the northwest). The image clearly shows the sharp edge of the surface brightness discontinuity, shaped by the ram pressure of the Fornax cluster gas. The temperature map (Fig. 3b) confirms that the infalling cloud is cold compared to the surrounding Fornax ICM.

Cold fronts provide a unique opportunity to explore cluster physics. In a study of A3667, Vikhlinin et al. (2001a, b) derived the ram pressure of the ICM on the moving cold front from the gas density and gas temperature. In turn, the ram pressure yielded a measurement of the cold front velocity. The factor of two difference in pressures between the free streaming region and the region immediately inside the cold front implied a cloud velocity of 1430 ± 290 km s^{-1} (Mach 1 ± 0.2). In addition, Vikhlinin et al. (2001b) showed that the "edge" of the cold front in A3667 is very sharp – the width of the front was less than $3.5''$ (5 kpc). This sharp edge requires that transport processes across the edge be suppressed, presumably by magnetic fields. Without such suppression, the density discontinuity at the "edge" would be broader since the relevant Coulomb mean free path for electrons is several times the width of the cold front.

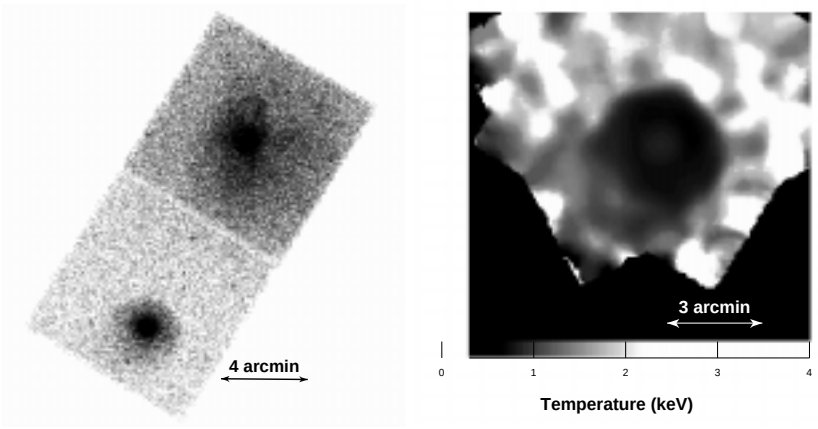

Figure 3. The ACIS observation of NGC1404 and NGC1399. (**a**) The 0.5–2.0 keV band image of the Fornax cluster. The gas filled dark halo surrounding NGC1404 is at the lower left (southeast) while the cluster core, dominated by the halo surrounding NGC1399 lies at the upper right (northwest). (**b**) The temperature map of the Fornax region. The cold core surrounding NGC1404 has a temperature of less ~ 1 keV while the surrounding gas has a temperature of $\gtrsim 1.5$ keV.

Furthermore, Vikhlinin et al. observed that the cold front appears sharp only over a sector of about $\pm 30^\circ$ centered on the direction of motion, while at larger angles, the sharp boundary disappears. The disappearance can be explained by the onset of Kelvin-Helmholtz instabilities, as the ambient ICM gas flows past the moving cold front. To suppress the instability over the inner $\pm 30^\circ$ requires a magnetic field parallel to the boundary with a strength of $7 - 16 \mu$G (Vikhlinin et al. 2001b).

1.3. A Classic Supersonic Merger - 1E0657

1E0657 ($z = 0.296$) was discovered by Tucker et al. (1995) as part of a search for "failed" clusters, clusters that were X-ray bright but had few, if any, optical galaxies. The cluster temperature, as measured from ASCA observations, was found to be remarkably high, about 17 keV, making it the hottest cluster known (Tucker et al. 1998).

The Chandra image of 1E0657 shows the classic properties of a supersonic merger (see Markevitch et al. 2002a for a detailed discussion). The image shows a dense (cold) core moving to the west after having traversed, and disrupted, the core of the main cluster. Leading the cold, dense core is a density discontinuity that appears as a shock front (Mach cone). The shock is confirmed by the spectral data since the gas to the east (trailing the shock) is hotter than that in front of the discontinuity, unlike the cold fronts discussed above (or the western boundary of the bullet which also is a cold front). The detailed gas density parameters confirm that the "bullet" is moving to the west with a velocity of 3000–4000 km sec^{-1}, approximately 2-3 times the sound speed of the ambient

gas. 1E0657 is the first, and so far the only, clear example of a relatively strong shock arising from cluster mergers.

2. Interaction between Hot Gas in Galaxies, Groups, and Clusters with Energy Produced by AGN Accretion

With the greatly increased observing capabilities provided by Chandra and XMM-Newton, the complexity of the phenomena exhibited by hot gas in early type galaxies, groups and clusters seen in X-rays has grown. Not only do we see the effects of merging, but also we see the detailed effects on the hot gaseous atmospheres of the liberation of accretion energy as relativistic plasmas are expelled from AGN.

One of the first, and clearest, examples of the effect of plasma bubbles on the hot intracluster medium was found in the Perseus cluster around the bright active, central galaxy NGC1275 (3C84). First studied in ROSAT images (Bohringer et al. 1993), the radio emitting cavities to the north and south of NGC1275 are clearly seen in the Chandra images with bright X-ray emitting rims surrounding the cavities that coincide with the inner radio lobes (Fabian et al. 2000). For NGC1275/Perseus, the radio lobes are in approximate pressure equilibrium with the ambient, denser and cooler gas and the bright X-ray rims surrounding the cavities are cooler than the ambient gas. The central galaxy in the Hydra A cluster also harbors X-ray cavities associated with radio lobes that also show no evidence for shock heating (McNamara et al. 2000). Both sets of radio bubbles, being of lower density than the ambient gas, must be buoyant.

The Chandra images of Perseus/NGC1275 also suggest the presence of older bubbles produced by earlier outbursts (Fabian et al. 2000). These older bubbles appear as X-ray surface brightness "holes", but unlike the inner bubbles, these outer holes show no detectable radio emission, suggesting that the synchrotron emitting electrons may have decayed away leaving a heated, plasma bubble (see Fabian et al. 2002a who reported low frequency radio spurs extending towards the outer bubbles in NGC1275, consistent with this scenario). Such bubbles, with no attendant radio emission, are seen by Chandra in the galaxy groups HCG62 and MKW3s (Vrtilek et al. 2001; Mazzotta et al. 2002).

In addition to bubbles associated with central dominant cluster galaxies, bubbles and their effects also are seen in more typical early type galaxies. For example, in the E1 galaxy M84 (NGC4374), Chandra observed an unusual X-ray morphology which is explained by the effect of the radio lobes on the hot gas (Finoguenov & Jones 2001). The X-ray emission appears $\mathcal{H}$-shaped, with a bar extending east-west with two nearly parallel filaments perpendicular to this bar. The complex X-ray surface brightness distribution arises from the presence of two radio lobes (approximately north and south of the galaxy) that produce two low density regions surrounded by higher density X-ray filaments. As with Perseus/NGC1275 and Hydra A, the filaments, defining the $\mathcal{H}$-shaped emission, have gas temperatures comparable to the gas in the central and outer regions of the galaxy and hence argue against any strong shock heating of the galaxy atmosphere by the radio plasma.

Although the bubbles are not driving shocks into the surrounding gas, they still can provide significant energy input. One particularly well-studied system

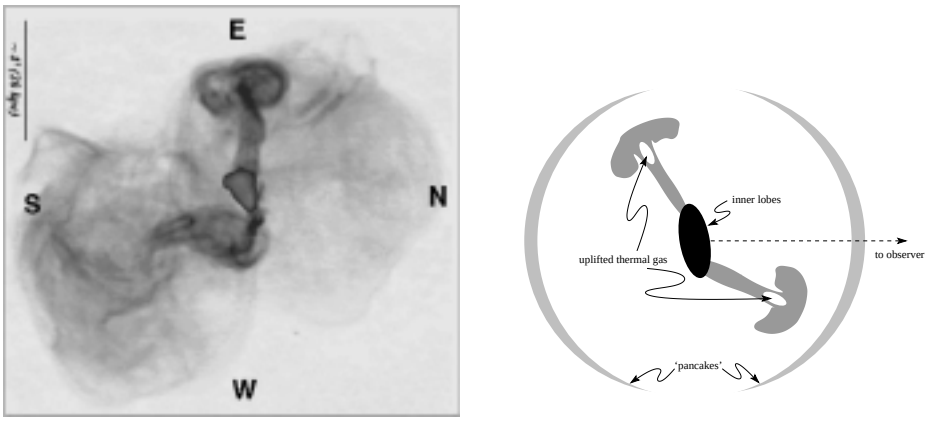

Figure 4. (**a**) $14'.6 \times 16'.0$ radio map of M87 (North to the right, East is up) (from Owen et al. 2000). (**b**) Source geometry. The central black region represents the inner radio lobes, the gray "mushrooms" correspond to buoyant bubbles, transformed into tori, and the gray lens-shaped structures are "pancakes" (seen edge-on) formed by older bubbles.

combining complex X-ray and radio emission is M87, at the center of the Virgo cluster. The 327 MHz high resolution, high dynamic range radio map of M87 (see Fig. 4a) shows a well-defined torus-like eastern bubble and a less well-defined western bubble, both of which are connected to the central emission by a column, and two very faint almost circular emission regions northeast and southwest of the center (Owen et al. (2000). The correlation between X–ray and radio emitting features has been remarked by Feigelson et al. (1987), Bohringer et al. (1995), and Harris et al. (1999).

Motivated by the similarity in appearance between M87 and hot bubbles rising in a gaseous atmosphere, Churazov et al. (2000) developed a simple model of the M87 bubbles which is generally applicable to the many bubble-like systems seen in the Chandra observations. An initial buoyant, spherical bubble transforms into a torus as it rises through the galaxy or cluster atmosphere. By entraining cool gas as it rises, it exhibits a characteristic "mushroom" appearance, similar to an atmospheric nuclear explosion. This may qualitatively explain the correlation of the radio and X–ray emitting plasmas and naturally accounts for the thermal nature of the X-ray emission associated with the rising torus (Bohringer et al. 1995). Ambient gas is uplifted in the cluster atmosphere producing the "stem" of the mushroom that is brighter than the surrounding regions (Churazov et al. 2000). Finally, in the last evolutionary phase, the bubble reaches a height at which the ambient gas density equals that of the bubble. The bubble then expands to form a thin layer (a "pancake"). The large low surface brightness features in the M87 radio map could be just such pancakes (see Fig. 4b for a schematic of the radio emitting components of M87).

The XMM-Newton observation (see Belsole et al. 2001) supports the buoyancy scenario with spectra showing that emission from the X-ray columns is

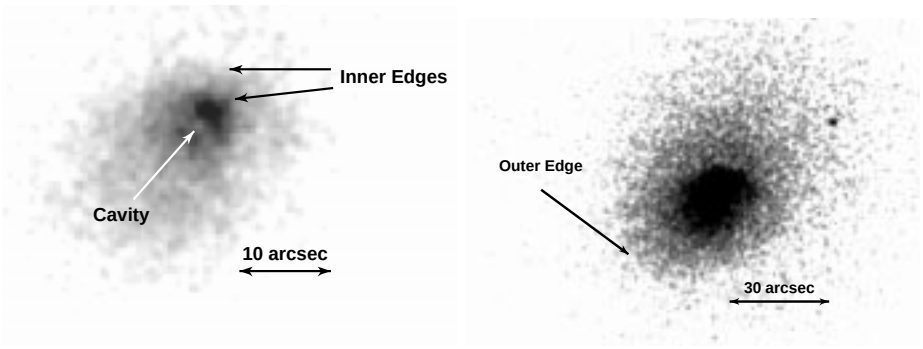

Figure 5. Edges in ZW3146. (**a**) The 0.5-2.0 keV image of the central region of ZW3146 shows two "edges" as well as an inner cavity at the position of a nuclear radio source which lies at the center of the optical image of the cD galaxy. (**b**) A third "edge" appears on a larger scale at $\sim 35''$ from the cD galaxy center.

thermal in nature with a gas temperature that is lower (1.5 keV) than the surrounding gas (2.3 keV).

2.1. ZW3146 - Multiple Edges

ZW3146 is a moderately distant ($z = 0.29$; 5.74 kpc per arcsec) cluster with a remarkably high mass deposition rate that has been estimated to exceed 1000 $M_\odot$ yr^{-1} (Edge et al. 1994). The Chandra image further demonstrates the remarkable nature of this cluster – on scales from $3''$ to $30''$ ($\sim$ 20 kpc to 170 kpc), three separate "edges" are detected (see Fig. 5 and Forman et al. 2003b). At the smallest radii, two edges are seen to the northwest and north (see Fig. 5a). The first, at a radius of $\sim 3''$ (17 kpc) has a surface brightness drop of almost a factor of 2. This innermost "edge" defines a cavity, surrounded by a partial shell, centered on the bright, central cD galaxy. The cavity probably arises as relativistic plasma (seen as radio emission in the NVSS/FIRST survey) produced in the central AGN expands outward and evacuates the X-ray emitting plasma from the immediate environs of the the nucleus. The second edge, at a radius of $\sim 8''$ (45 kpc) has a surface brightness drop of almost a factor of 4. The third "edge" (Fig. 5b) lies to the southeast, about $35''$ (200 kpc) from the cluster center. One possibility for the origin of these multiple edges is that the $8''$ edge is produced by gas motions induced by the expanding plasma bubble in the central core. Alternatively, "sloshing" motions can arise either from mergers or bubbles (e.g., Markevitch et al. 2001; Churazov et al. 2003).

Studies of clusters like ZW3146, for which the standard cooling flow scenario predicts large mass deposition rates but which have complex cores, may help to resolve the source of the energy needed to moderate the effects of radiative cooling as required by recent XMM and Chandra observations (e.g., Peterson et al. 2001 and Tamura et al. 2001). A variety of proposals have been made to explain the much smaller amounts of cool gas than expected (e.g., Churazov et al. 2001, Bruggen & Kaiser 2001, Quilis et al. 2001, Bohringer et al. 2002, Nulsen et al. 2002, Fabian et al. 2002b, 2002c, Ruszkowski & Begelman 2002,

Zakamska & Narayan 2002, Churazov et al. 2002). Only more observational studies can determine which processes are most effective.

2.2. Origin of Density Edges

The variety of morphologies and scales exhibited by sharp edges or cold fronts seen in Chandra images is quite remarkable. Possibly the edges may arise from moving cold gas clouds that are the remnants of merger activity. They may arise either from massive mergers as in A2142, multiple collapses as suggested for RXJ1720.1+2638 (Mazzotta et al. 2001), or gas oscillations (sloshing) in "cooling flow" clusters (Markevitch et al. 2001, 2002b). For A3667, the data were of sufficiently high quality that the parameters of the dark matter halo associated with the observed gas cloud could be derived (Vikhlinin & Markevitch 2002). Alternatively, some edges could arise from the interaction of surviving cold, dark matter halos as they move within the cluster potential. High resolution, large scale structure simulations show that dense dark matter halos, formed at very early epochs, would not be disrupted as clusters collapse (Ghigna et al. 1998 and Ghigna et al. 2000). While most of the dark matter halos, having galaxy size masses, are associated with the sites of galaxy formation, larger mass halos also may survive or may have fallen into the cluster only recently. Hence, we might expect to find a range of halo mass distributions moving within the cluster potential. As these halos move, they could give rise to the multiple surface brightness edges observed in some clusters. Churazov et al. (2003) showed that edges/cold fronts in cluster cores could be produced by weak shocks or sound waves as they traverse cluster cores. Such waves can be generated by infalling gas that provides an impetus to the core gas. The infalling gas itself does not penetrate the core. A crude simulation of such a scenario was used by Churazov et al. (2003) to explain the appearance of the core of the Perseus cluster. Still another possible mechanism to generate edges in cluster (or group or galaxy) atmospheres is from motions induced by buoyant bubbles of relativistic particles produced in central AGN (Quilis et al. 2001, Churazov et al. 2001). Buoyant bubbles can entrain, uplift and possibly drive gas motions. Thus, a variety of physical mechanisms have been suggested to produce the observed cold fronts/edges. Probably, at least several of these mechanisms are operative in different clusters and perhaps even in the same cluster where mergers are underway and AGN in the central galaxies are producing relativistic plasma bubbles.

2.3. Explosive Cavities

NGC4636 is one of the nearest and most X-ray luminous "normal" elliptical galaxies (L_X $\sim$2$\times$10^{41} ergs s^{-1}). The first X-ray imaging observations of NGC4636 from Einstein showed that, like other luminous elliptical galaxies, NGC4636 was surrounded by an extensive hot gas corona (Forman, Jones & Tucker 1986).

The Chandra observation of NGC4636 shows a new phenomenon – shocks produced by nuclear outbursts (see Jones et al. 2002 for details of the Chandra observation of NGC4636). The high angular resolution Chandra image (see Fig. 6) shows symmetric, $\sim$ 8 kpc long, arm-like features in the X-ray halo surrounding NGC4636. The leading edges of these features are sharp and are

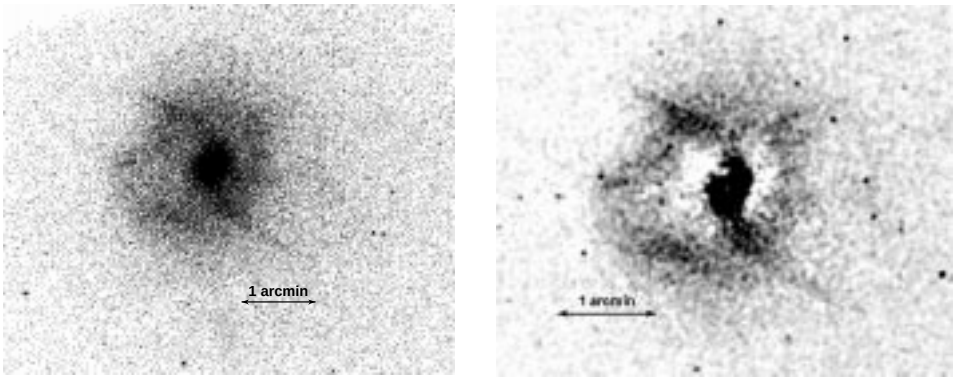

Figure 6. (**a**) The 0.5-2.0 keV ACIS-S image of NGC4636. (**b**) The smoothed emission after an azimuthally symmetric model describing the galaxy corona has been subtracted. Shocks from a recent nuclear outburst could produce the brighter arm-like structures, while the additional features could arise from other outbursts.

accompanied by temperature increases of $\sim 30\%$, as expected from shocks propagating in a galaxy atmosphere.

Although the sharpness of the edges of the NE and SW arms appears similar to the sharp edges found along "fronts" in clusters (see discussion and references above), the cluster "fronts" are cold, while those in NGC4636 are hot. Also, while the presence of sharp fronts suggests the possibility of an ongoing merger, the east-west symmetry of the halo structures, the similarity of this structure to that seen around radio lobes, as well as the lack of a disturbed morphology in the stellar core or in the stellar velocities suggest an outburst from the nucleus as the underlying cause. In particular, the bright SW arm, the fainter NW arm and the bright NE arm can be produced by the projected edges of two paraboloidal shock fronts expanding about an east – west axis through the nucleus. A shock model is also consistent with the evacuated cavities to the east and west of the central region.

The size, symmetry, and gas density and temperature profiles of the shocks are consistent with a nuclear outburst of energy $\sim 6 \times 10^{56}$ ergs having occurred about $\sim 3 \times 10^6$ years ago. It is tempting to suggest that these outbursts are part of a cycle in which cooling gas fuels nuclear outbursts that periodically reheat the cooling gas. Such outbursts if sufficiently frequent could prevent the accumulation of significant amounts of cooled gas in the galaxy center.

3. Conclusions

We have described several of the new phenomena observed with Chandra and XMM-Newton. Of particular note are the density "edges" (some of which are shock fronts but most of which are cold fronts) and bubbles. Some cold fronts are certainly produced through mergers. However, others may arise from residual gas "sloshing" in cluster cores (Markevitch et al. 2002). The gas motions may be initiated by rising buoyant bubbles, weak sound waves traversing the cluster core,

or motions of dark matter halos that have survived mergers. Buoyant bubbles of relativistic plasma can induce complex morphologies in cluster (and group and galaxy) atmospheres as well as moderate the effects of radiative cooling. We have observed at least one example of an outburst (NGC4636) with direct heating of the surrounding gaseous atmosphere. Clearly, cluster cores are more complex than previous lower angular resolution observations had shown. Studies of this "complexity" provide a unique opportunity to better understand the details of cluster mergers and to investigate the interaction of relativistic plasma produced by AGN with the gas in the cluster cores.

We acknowledge support from NASA grant NAG5-9217 and NASA contract NAS8-39073.

References

Belsole, E. et al. 2001, A&A, 365, L188

Bohringer, H. et al. 1993, MNRAS, 264, L25

Bohringer, H., Nulsen, P., Braun, R., Fabian, A. 1995, MNRAS, 274, L67

Bohringer, H. et al. 2002, A&A, 382, 804

Bruggen, M. & Kaiser, C. 2001, MNRAS, 325, 676

Churazov, E, Forman, W., Jones, C., Bohringer, H. 2000, A&A,, 356, 788

Churazov, E., Bruggen, M., Kaiser, C., Bohringer, H. & Forman, W. 2001, ApJ, 554, 261

Churazov, E., Sunyaev, R., Forman, W. & Bohringer, H. 2002, MNRAS, 332, 729

Churazov, E. et al. 2003, ApJ submitted

Dosaj, A. et al. 2002, AAS, 200, 4317

Durret, F. et al. 1998, A&A,, 335, 41

Durret, F., Lima-Neto, G., Forman, W., Churazov, E. 2003, submitted to A&A

Edge, A. et al. 1994, MNRAS,, 270, L1

Fabian, A. et al. 2000, MNRAS, 318, L65

Fabian, A. C., Celotti, A., Blundell, K. M., Kassim, N. E., Perley, R. A. 2002a, MNRAS, 331, 369

Fabian, A. et al. 2002b, MNRAS, 332, L50

Fabian, A., Voight, M., Morris, R. 2002c, MNRAS, 335, L71

Feigelson, E. Wood, P. Schreier, E., Harris, D., Reid, M. 1987, ApJ, 312, 101

Finoguenov, A. & Jones. C. 2001, ApJL, 547, L107

Forman, W., Jones, C. & Tucker, W. 1986, ApJ, 300, 836

Forman, W. et al. 2003a, in preparation

Forman, W. et al. 2003b, submitted to ApJ

Ghigna, S., Moore, B., Governato, F., Lake, G., Guinn, T., Stadel, J. 1998, MNRAS,, 300, 146

Ghigna, S., Moore, B., Governato, F., Lake, G., Guinn, T., Stadel, J. 2000, ApJ, , 544, 616

Jones, C., Forman, W., Vikhlinin, A. Markevitch, M., David, L., Warmflash, A. Murray, S., Nulsen, P. 2002, ApJL, 567, L115

Kempner, J., Sarazin, C. & Ricker, P. 2002, ApJ. 579, 236

Markevitch, M. et al. 2000, ApJ, 541, 542

Markevitch, M., Vikhlinin, A., Mazzotta, M. 2001, ApJL, 562, L153

Markevitch, M. et al. 2002a, ApJL, 567, L27

Markevitch, M., Vikhlinin, A., Forman, W. 2002b, ASP Proceedings, astro-ph/0208208

Matsumoto, H. et al. 1997, ApJ, 482, 133

Mazzotta, P. et al. 2002, ApJL, 567, L37

Mazzotta, P. et al. 2001, ApJ, 555, 205

McNamara, B. et al. 2000, ApJL , 534, 135

Nulsen, P. et al. 2002, ApJ, 568, 163

Owen, F., Eilek, J., Kassim, N. 2000, ApJ, 543, 611

Quilis, V., Bower, R. & Balogh, M. 2001, MNRAS, 328, 1091

Ruszkowski, M. & Begelman, M. 2002, ApJ, 581, 223

Tucker, W., Tananbaum, H., & Remillard, R. 1995, ApJ, 444, 532

Tucker, W. et al. 1998, ApJ, 496, L5

Van Haarlem, M. & Van de Weygaert, R. 1993, ApJ, 418, 544

Vikhlinin, A., Markevitch, M., Murray, S. 2000a, ApJ, 551 160

Vikhlinin, A., Markevitch, M., Murray, S. 2000b, ApJ, 549, L47

Vikhlinin, A. & Markevitch, M. 2002, Astr. Letters, 28, 495

Vrtilek, J. et al. 2001, IAP Workshop (2001)

West, M. & Blakeslee, J. 2000, ApJ, 543, L27

Zakamska, N. & Narayan, R. 2002, ApJ, 582, 162